Nanoscale Advances

ROYAL SOCIETY OF CHEMISTRY

REVIEW

View Article Online
View Journal | View Issue

Cite this: *Nanoscale Adv.*, 2025, **7**, 4763

Nano-enhanced Fenton/Fenton-like chemistry: integrating peroxidase nanozymes, MOFs, and MXenes for next-generation colorimetric biosensors

Hanh An Nguyen, †[a] Nguyen Tran Truc Phuong, †[bc] Nguyen Bao Tran,[de] Thi Ngoc Diep Trinh,[f] Ngoc Xuan Dat Mai,[eg] Ngoc Quang Tran,[eg] Nhu Hoa Thi Tran *[de] and Kieu The Loan Trinh *[eg]

Received 22nd April 2025
Accepted 27th June 2025

DOI: 10.1039/d5na00387c

rsc.li/nanoscale-advances

Colorimetric biosensors exhibit promising potential toward molecular analysis with a wide range of sample types such as clinical, environmental, animal, and plant samples due to their high portability, sensitivity, specificity, and accuracy. Colorimetric biosensors rely on chromogenic reactions to transduce biochemical signals into visible color changes. Among the various signal transduction mechanisms, the Fenton/Fenton-like reaction is an outstanding reaction that can be used to detect a broad spectrum of analytes under diverse conditions. The ability to detect a wide range of analytes expands the application of the Fenton/Fenton-like reaction; this comes at the cost of specificity. This review highlights how integrating nanomaterials, such as peroxidase nanozymes, metal–organic frameworks (MOFs), and MXenes, can improve conventional Fenton/Fenton-like reactions, significantly enhancing specificity, selectivity, and catalytic efficiency. Besides, we demonstrated that the terms "Fenton/Fenton-like reaction" and "peroxidase-mimic nanozyme activity" fundamentally describe the same catalytic process, providing a unified perspective for researchers in the field. Moreover, the incorporation of MOFs and MXenes offers abundant active sites and

[a]*Department of Molecular Biology, Institute of Food and Biotechnology, Can Tho University, Can Tho City, Vietnam*
[b]*Nguyen Tat Thanh University Center for Hi-Tech Development, Saigon Hi-Tech Park, Ho Chi Minh City, Vietnam*
[c]*NTT Hi-Tech Institute, Nguyen Tat Thanh University, Ho Chi Minh City, Vietnam*
[d]*Faculty of Materials Science and Technology, University of Science, Ho Chi Minh City 70000, Vietnam. E-mail: ttnhoa@hcmus.edu.vn*
[e]*Vietnam National University, Ho Chi Minh City 70000, Vietnam*
[f]*BioTechnology Institute, Tra Vinh University, Tra Vinh City 87000, Vietnam*
[g]*Center for Innovative Materials and Architectures, Ho Chi Minh City 70000, Vietnam. E-mail: tktloan@inomar.edu.vn*
† These authors contributed equally to this work.

Hanh An Nguyen

Dr Hanh An Nguyen received her BS degree from the Biotechnology Research and Development Institute at Can Tho University, Vietnam, in 2019 and her ME (2021) and PhD (2024) from the Department of BioNano Technology at Gachon University in Korea. Her research interests include the development of miniaturized biosensors for monitoring analytes, POCT, and nanomaterials. Currently, she works in the Department of Molecular Biology, Institute of Food and Biotechnology at Can Tho University as a researcher.

Nguyen Tran Truc Phuong

Ms Nguyen Tran Truc Phuong received a BSc degree (2021) in thin film and nanomaterials sciences from the Faculty of Materials Science and Technology and an MSc degree (2024) from the Faculty of Materials Science at the University of Science, Vietnam National University, Ho Chi Minh City. She also works at the NTT Hi-Tech Institute, Nguyen Tat Thanh University, Ho Chi Minh City, Vietnam. Her main research interests are nanomaterials, colorimetric sensors, surface plasmon resonance (SPR) enhancement, surface-enhanced Raman scattering (SERS), and optical fiber sensors.

enhanced electron transfer, resulting in improved sensitivity and selectivity in Fenton-based colorimetric assays.

1. Introduction

Colorimetric biosensors hold significant promise for molecular analysis and are widely utilized in clinical diagnostics, environmental monitoring, and quality control in the food industry. Colorimetric biosensors meet the urgent needs of on-field target monitoring due to the ability to operate outside the laboratory, simple fabrication, fast detection, and equipment-free result readout. The outstanding performance of colorimetric biosensors has been demonstrated in terms of high sensitivity, specificity, and portability. Their detection principle is based on chromogenic reactions, where the presence of target analytes triggers conformational changes in chromogenic substrates or influences chromogenic reactions, leading to distinct color shifts in the solution.[1–3]

Most well-known chemical reactions for colorimetric detection include the Fenton/Fenton-like reaction, Schiff's base reaction, Lowry reaction, Bradford reaction, and plasmonic effects.[4–9] Among them, the Fenton/Fenton-like reaction stands out as a particularly promising approach for several reasons. First, the Fenton/Fenton-like reaction can be used to detect a wide range of analytes such as metal ions, proteins, nucleic acids, and microorganisms, whereas the Schiff's base reaction, Lowry reaction, and Bradford reaction only detect aldehydes or proteins. Second, in contrast to plasmonic effects, which rely on limited types of materials, the Fenton/Fenton-like reaction can be initiated by a wide range of reagents, making it highly adaptable for different sensing applications. Given these advantages, this reaction holds great potential for the development of colorimetric biosensors. However, the Fenton/Fenton-like reaction still has some

Nguyen Bao Tran

Ms Nguyen Bao Tran is currently studying at the Faculty of Materials Science and Technology, University of Science, Vietnam National University, Ho Chi Minh City, Vietnam (2021–2025). She is working in the Optics and Sensors Group at the Faculty of Materials Science and Technology, University of Science, Vietnam National University, Ho Chi Minh City. Her main research interests are surface plasmon resonance (SPR), surface-enhanced Raman scattering (SERS), fiber-optic sensors, and optical biosensors.

Thi Ngoc Diep Trinh

Dr Thi Ngoc Diep Trinh received a PhD from Gachon University, South Korea, in 2019. In 2020, she was appointed as an Assistant Professor at Gachon University, South Korea. She has been a lecturer at the Biotechnology Institute, Tra Vinh University, Vietnam, since 2023. Her major research interests include loop-mediated isothermal amplification, antibiotic-resistant microorganisms, and point-of-care testing.

Ngoc Xuan Dat Mai

Dr Ngoc Xuan Dat Mai received his PhD degree in Optics from the University of Science, Vietnam National University, Ho Chi Minh City. He is a researcher at the Center for Innovative Materials and Architectures (INOMAR), Vietnam National University – Ho Chi Minh City. His research interests include the synthesis and applications of porous materials for drug delivery, biosensors, photocatalysts, and bioimaging.

Ngoc Quang Tran

Dr Ngoc Quang Tran is a group leader at the Center for Innovative Materials and Architectures (INOMAR), a member of Vietnam National University, Ho Chi Minh City. He earned his doctoral degree from Sungkyunkwan University, South Korea, in 2019. He was a postdoctoral researcher at the Center for Integrated Nanostructure Physics, Institute for Basic Science (IBS), Sungkyunkwan University, South Korea, from 2019 to 2021. His research focuses on synthesis and chemical engineering of non-noble metal nanomaterials for energy storage and conversion devices such as electrochemical water splitting, electrochemical supercapacitors, and metal ion batteries.

limitations that need to be overcome. For instance, the ability to respond to broad analytes expands its application; nevertheless, this comes at the cost of reduced specificity.[10–13]

The latest advancements in nanotechnology have created a fresh window of opportunity to improve the limitations of the Fenton/Fenton-like reaction. By leveraging nanotechnology, the analytical performance of the Fenton/Fenton-like reaction can be impressively enhanced through decreasing the size of Fenton/Fenton-like reagents down to the nanoscale, where unique quantum effects emerge, thereby increasing their catalytic activity. Unlike the traditional Fenton/Fenton-like reaction, which depends on strongly acidic conditions to trigger the reaction and has poor molecular accessibility, the nanoscale Fenton/Fenton-like reaction has mild reactive conditions and high molecular accessibility. For example, Meng *et al.* synthesized a ferric hydroxide nanocage ($Fe(OH)_3$-NC) to trigger the Fenton/Fenton-like reaction, which was applied for the detection of CA 19-9, a model analyte.[14] $Fe(OH)_3$-NC the triggered Fenton/Fenton-like reaction under neutral pH conditions and provided more accessible catalytic sites, resulting in increasing analytical performance. Liang *et al.* used a Cu-Fenton system, mimicking peroxidase activity for colorimetric detection of creatinine.[13] This research demonstrated that the distinction between the 'Fenton/Fenton-like reaction' and 'peroxidase activity' can be conceptually merged, especially within the framework of colorimetric biosensing. This conceptual merging enables the application of recent advantages from both systems to enhance the design and performance of colorimetric biosensors. Furthermore, along with significant advances in nanotechnology, tailorable nanomaterials can be rationally designed to enable the Fenton/Fenton-like reaction in response to specific analytes. Metal–organic frameworks (MOFs), for example, offer tunable porosity, allowing precise control over pore sizes and geometries to selectively bind target analytes. This not only enhances selectivity but also minimizes interference from non-specific molecules.[15,16] Moreover, the stability of the Fenton/Fenton-like reaction can be improved when Fenton/Fenton-like reagents are anchored onto nanomaterials. MXenes, with a unique accordion structure, large surface area, and abundant terminal groups, serve as excellent nanomaterials for anchoring and stabilizing Fenton/Fenton-like reagents.[17,18]

In this review, the mechanisms of the Fenton/Fenton-like reaction for catalyzing colorimetric detection are first described. Then, the role of nanotechnology in improving the Fenton/Fenton-like reaction for colorimetric biosensor applications is discussed.

2. Principle of the Fenton/Fenton-like reaction

Initially, in 1876, Henry John Horstman Fenton discovered the special feature of ferrous ions (Fe^{2+}) allowing them to oxidize tartaric acid ($C_4H_6O_6$) with enhanced activity in the presence of hydrogen peroxide (H_2O_2). This catalytic oxidation system was then named after him as the Fenton reagent. Afterwards, finding the mechanism of the reagent he discovered became his career goal. Unfortunately, Fenton died in 1929 without knowing the mechanism fully explaining the Fenton reaction.[19,20] Following Fenton's work, Fritz Haber and Joseph Weiss explained the mechanism of the Fenton reaction involving the generation of hydroxyl radicals ($^{\bullet}OH$) in H_2O_2 reduction by Fe^{2+}.[21] They proposed that the Fe^{2+} ion donates an electron to an H_2O_2 molecule resulting in the generation of $^{\bullet}OH$ through cleaving the O–O bridge of H_2O_2. The $^{\bullet}OH$ radical then reacts with another

Nhu Hoa Thi Tran

Dr Nhu Hoa Thi Tran received a BSc degree (2011) in thin film and nanomaterials science from the Faculty of Materials Science and Technology, and an MSc degree (2014) in physics and engineering physics from the University of Science, Vietnam National University, Ho Chi Minh City. She received her DPhil from the Department of Nano Science and Technology, College of BioNano Technology, Gachon University, the Republic of Korea, in 2018, and became an assistant professor in the Department of Nano-Physics, Gachon University, the Republic of Korea (2018). Now, she is working in the Faculty of Materials Science and Technology, University of Science, Vietnam National University, Ho Chi Minh City. Her main research interests are in surface plasmon resonance (SPR)-enhanced fluorescence for PCR, optical biosensors, bio-nanophotonics, and their applications in biomedical optical fiber sensors.

Kieu The Loan Trinh

Dr Kieu The Loan Trinh received her BS degree from the Biotechnology Research and Development Institute at Can Tho University, Vietnam, in 2010 and her ME (2012) and PhD (2015) in the Department of BioNano Technology at Gachon University in Korea. Currently, she works at the Center for Innovative Materials and Architectures (INOMAR), Vietnam National University, Ho Chi Minh City (VNU-HCM), as a researcher. Her research interests include the development of miniaturized devices for genetic analyses, system integration, POCT, biosensors, nanomaterials, and biomaterials.

H_2O_2 molecule to generate superoxide ($O_2^{\bullet -}$) and eventually form oxygen. The reaction chain is summarized below.

$$HOOH + M^{+x} \rightarrow HO^{\bullet} + M^{(+x+1)} + OH^{-} \quad (1)$$

$$HO^{\bullet} + HOOH \rightarrow H_2O + HO_2^{\bullet} \quad (2)$$

$$HOOH + HO_2^{\bullet} \rightarrow HO^{\bullet} + O_2 \quad (3)$$

$$HOOH \xrightarrow{\gamma/UV} HO^{\bullet} + HO^{\bullet} \quad (4)$$

$$HO^{\bullet} + RH \rightarrow R^{\bullet} + H_2O \quad (5)$$

$$HO^{\bullet} + R^{\bullet} \rightarrow R{-}OH \quad (6)$$

$$R^{\bullet} + R^{\bullet} \rightarrow R{-}R \quad (7)$$

where M represents metals.

The hydroxyl radicals, which are generated in the Fenton reaction, have an extremely strong oxidation activity with oxidation potential varying between ~2.0 and 2.8 E° (V). Thus, hydroxyl radicals are placed between ozone and fluorine among common oxidants.[22] With the strong oxidation feature, the Fenton reaction has been widely used to degrade organic pollutants such as phenols, pesticides, pharmaceuticals, organic solvents, organic dyes, *etc.* Furthermore, the Fenton reaction has attracted great interest due to the rapid reaction, cheap and easy-to-find chemicals, and the ability to operate at ambient pressure and temperature. Recently, the application of the Fenton reaction has been extended to colorimetric assays for target analysis through employing the ability to rapidly react with organic dyes. In colorimetric assays, the Fenton reaction is commonly used to oxidize 3,3′,5,5′-tetramethylbenzidine (TMB)—a chromogenic substrate. The mechanism of this reaction involves a reaction between the surface Fe^{2+} (oxidation) and H_2O_2 (reduction) to generate $^{\bullet}OH$ and Fe^{3+}. Then, the resultant $^{\bullet}OH$ participates in the oxidation of TMB, which causes a perceptible change from colorless to blue (Fig. 1).[23] The presence of targets interrupts or enhances the effect of the Fenton reaction on TMB, resulting in altering the original color-changing trend. Guo *et al.* reported that Fe_3O_4 first forms an intermediate with H_2O by capturing an O atom from a H_2O_2 molecule.[24] Then, TMB binds to the surface of Fe_3O_4–O* and donates an electron to the exposed O atom to form an Fe_3O_4–O–TMB complex. In this step, TMB is oxidized, while Fe_3O_4–O* is reduced to form an Fe_3O_4–OH–oxTMB complex. oxTMB then leaves this complex resulting in Fe_3O_4–OH formation. Another TMB molecule approaches the Fe_3O_4–OH structure to form an Fe_3O_4–OH–TMB complex, which in turn creates another oxTMB and water molecule, while Fe_3O_4 is regenerated. In short, a cycle of this catalysis consumes one H_2O_2 molecule to oxidize two TMB molecules and form two H_2O. Although the reaction of surface Fe^{2+} is the key process accounting for generating $^{\bullet}OH$, internal atomic changes and their contribution to the catalytic reaction should not be underestimated. Recently, Dong *et al.* proved that the electrons can be transferred from the internal Fe^{2+} within Fe_3O_4 to the surface through the Fe^{2+}–O–Fe^{3+} chain, resulting in the regeneration of Fe^{2+}.[25] Since the Fenton reaction can occur with a variety of chromogenic substrates, Fenton reaction-based colorimetric assays can be expanded by using other chromogenic substrates such as *o*-phenylenediamine (OPD),[26] 2,2′-azinobis(3-ethylbenzothiazoline-6-sulfonic acid) diammonium salt (ABTS),[27] 3,3′-diamino benzidine (DAB),[28] *etc.* These substrates can produce colored products during target analysis.

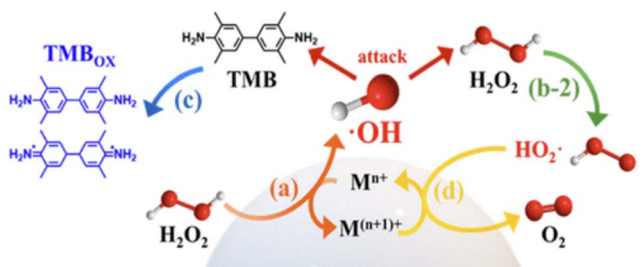

Fig. 1 Schematic diagram showing the color shift effect *via* the Fenton reaction.[23]

Modifications and improvements to the traditional Fenton reaction have been investigated aiming to increase reaction kinetics and enhance catalysis reactivity. Measures to achieve the improvement include the usage of alternative reagents to replace iron ions. Such reagents are commonly multivalent metals such as Cu, Mn, Co, Ce, Ag, Cr, Ru, Mo, V, W, Ti, *etc.*[29,30] Like Fe ions, these metal ions can react with H_2O_2 to generate $^{\bullet}OH$. The reactions of these alternative reagents with H_2O_2 are referred to as Fenton-like reactions. Lower valent metals (M^{n+}) possess reduction properties and are converted to higher valent metals ($M^{(n+x)+}$) with oxidation properties. Meanwhile, H_2O_2 possesses both reduction and oxidation properties. Although higher valent metals can also react with H_2O_2 to generate $^{\bullet}OH$, the reaction rate is quite low as compared to that of lower valent metals. Thus, the regeneration of lower valent metals from higher valent metals is essentially important. Other oxidants such as peroxymonosulfate (PMS)[31] and peroxydisulfate (PDS)[32] are alternative options for replacing H_2O_2 in the Fenton/Fenton-like reaction. The positively charged catalytic metal center can form complexes with the electronegative oxygen atoms in the peroxyl O–O bond of the peroxide family (H_2O_2, PMS, PDS, *etc.*). Due to their multivalent nature and lower electronegativity (X_{TM} = 1.36–2.54) compared to O (X_O = 3.44),[33] transition metals can activate the O–O bond. Subsequently, electrons migrate from metal sites to peroxide, resulting in the breaking of the O–O bond and $^{\bullet}OH$ generation. The decomposition of H_2O_2 (HO–OH) by the Fenton/Fenton-like reaction generates $^{\bullet}OH$, while the decomposition of PMS (HO–O–SO_3–) and PDS (–O_3S–O–O–SO_3–) generates $^{\bullet}OH$ and/or $SO_4^{\bullet -}$.[34]

3. Fenton/Fenton-like reaction coupling with nanotechnology for colorimetric biosensors

3.1. Fenton/Fenton-like reaction and peroxidase-mimic nanozyme: the two different terminologies describing the same fundamental catalytic process

The Fenton/Fenton-like reaction shares a fundamental mechanism with peroxidase-mimic enzymes, as they both generate

reactive oxygen species (ROS) as the major products that play a vital role in colorimetric biosensors. Both systems rely on the reaction between transition metals and H_2O_2 to generate ROS such as $^{\bullet}OH$ and $O_2^{\bullet-}$ stimulating oxidation of chromogenic substrates. Peroxidase-mimic nanozymes describe a context in nanotechnology, which is involved in nanomaterials that exhibit similar catalytic activity to natural peroxidase. Meanwhile, the traditional Fenton/Fenton-like reaction is a term relating to homogeneous or heterogeneous catalysis, where the oxidation states of metal ions are cycled to degrade H_2O_2 into $^{\bullet}OH$. Although peroxidase-mimic nanozymes are described using different terminology, the underlying chemistry remains the same. That is related to the generation of $^{\bullet}OH$ and other types of ROS through the decomposition of H_2O_2 driven by transition metals, which subsequently oxidizes chromogenic substrates in colorimetric biosensors.[35]

The distinction between the Fenton/Fenton-like reaction and peroxidase-mimic nanozymes primarily arises from differences in research fields rather than fundamental chemistry. The term "peroxidase-mimic nanozymes" is used to describe a concept in nanotechnology that emphasizes the enzyme-like catalytic activity of nanomaterials, making them more convenient than natural peroxidase. Nevertheless, at its core, the working principle underlying peroxidase-mimic nanozymes is essentially a nanoscale adaptation of the Fenton/Fenton-like reaction. Moreover, both the Fenton/Fenton-like reaction and peroxidase-mimic nanozymes share one more similar reaction pathway regarding $O_2^{\bullet-}$ generation as the secondary product, further reinforcing their mechanistic overlap.[36] Therefore, rather than separating the Fenton/Fenton-like reaction and peroxidase-mimic nanozymes as distinct phenomena, they should be considered as the different terminologies describing the same fundamental catalytic process, one from the chemical viewpoint and the other from the nanomaterial engineering perspective. By doing this, the advantages and recent developments in both systems can be considered to improve colorimetric biosensors.

As a class of nanomaterials, nanozymes possessing intrinsic enzyme-mimic properties have been booming over the last decade due to their potential to overcome the limitations of traditional enzyme-based colorimetric assays. Along with the development of nanotechnology, nanozymes have superior properties over traditional enzymes regarding the capability to be rationally designed at the active centers and the surface. To date, nanozymes can mimic peroxidase, catalase, oxidase, superoxide dismutase, uricase, haloperoxidase, glutathione peroxidase, *etc.* However, only peroxidase-mimic nanozymes employ the Fenton/Fenton-like reaction. Therefore, this section mainly discusses peroxidase-mimic nanozymes.

3.1.1. Peroxidase-mimic nanozymes based on the Fenton reaction. The intrinsic peroxidase-like activity of Fe_3O_4 nanoparticles was first discovered by Gao *et al.* in 2007.[37] Since then, peroxidase-mimic nanozyme synthesis and their extensive applications have gathered attention from the scientific community, especially for colorimetric analysis. Fe_3O_4 nanozymes follow the ping-pong mechanism and Michaelis–Menten kinetics. This reaction mechanism is also called the non-sequential mechanism, which is characterized by the change in the nanozyme into an intermediate form due to the binding of the first substrate. The reaction proceeds with the reaction of the intermediate nanozyme with the second substrate. In this mechanism, one or more products are released before all substrates bind to the nanozyme.[38] Upon the addition of H_2O_2, Fe^{2+} is first converted into Fe^{3+} and $^{\bullet}OH$ is released. The as-produced Fe^{3+} and $^{\bullet}OH$ cause a perceptible change in TMB color from colorless to blue. Fe_3O_4 nanozymes are commonly applied for colorimetric H_2O_2 sensing platforms. The presence of H_2O_2 triggers the cycle of Fe^{2+}/Fe^{3+} releasing $^{\bullet}OH$ resulting in the production of colored TMB. However, like the traditional Fenton reaction, the redox cycle of Fe^{2+}/Fe^{3+} could be easily restricted because of the lower reaction rate of Fe^{3+} with H_2O_2, which can reduce the reaction rate in colorimetric H_2O_2 sensing. Baye *et al.* used an Fe_3O_4–Fe^0/Fe_3C nanozyme to overcome this limitation.[39] Fe^0/Fe_3C exhibits a fast Fe^{2+}/Fe^{3+} cycle in Fe_3O_4 particles increasing the probability and rate of decomposition of H_2O_2 into $^{\bullet}OH$. Fe^0/Fe_3C improves the Fe^{2+}/Fe^{3+} redox cycle, while the strong Lewis acid properties of Fe^{3+} enhance the adsorption of TMB. These synergistic effects of the Fe_3O_4–Fe^0/Fe_3C nanozyme enhance the sensitivity with a limit of detection (LOD) of 67.1 pM H_2O_2. Another strategy to upgrade the catalytic activity of Fe_3O_4 is using carbon supports such as AC-Fe_3O_4,[40] Fe_3O_4/N-doped PCNC,[41] GO-Fe_3O_4,[42] Fe_3O_4/carbon,[43] *etc.* Zeng *et al.* reported a library of single-atom (M_1-NC; 6 types) and dual-atom (M_1/M_2-NC; 13 types) metal–nitrogen–carbon nanocomposites (M = Fe, Co, Ni, Mn, Ru, Cu) to reveal peroxidase-like activities.[44] Among them, the Fe_1Co_1-NC dual-atom nanozyme with Fe_1–N_4/Co_1–N_4 coordination possessed the highest peroxidase-like activity. Density functional theory calculations showed that the d-band center position of the Fe atom site is synergistically affected by the Co atom site. Also, the Co atom acts as the second active site, which enhances peroxidase activity. In addition, a synergistic effect can be created by combining Fe_3O_4 with other metal or metal oxide nanoparticles. For example, He *et al.* synthesised core (Fe_3O_4)–shell (Pt) magnetic nanoparticles (Fe_3O_4@Pt NPs).[45] The peroxidase-like activity of Fe_3O_4@Pt NPs was 1.2 times and 2.6 times higher than that of Pt NPs and Fe_3O_4 NPs, respectively. Wang *et al.* combined Ag and Fe_3O_4 to generate Ag–Fe_3O_4 nanoparticles.[46] The K_m value of Ag–Fe_3O_4 for TMB was 4.2-fold lower than that of the single Fe_3O_4 nanozyme, indicating that Ag–Fe_3O_4 had higher affinity for TMB than the Fe_3O_4 nanozyme. Other possible combinations are Au–Fe_3O_4,[47] Zn–Fe_3O_4,[48] Cu–Fe_3O_4,[49,50] Cu_2O–Fe_3O_4,[51] Co–Fe_3O_4,[52] Mg–Fe_3O_4,[53] *etc.* The peroxidase-like activity not only depends on the composition but also depends on the nanocrystal morphology. Zhong *et al.* synthesized Fe_3O_4 nanocrystals with five different morphologies and compared their Fenton catalytic activity.[54] As a result, the Fenton activity of the as-prepared Fe_3O_4 was in the sequence of nanospheres > nanoplates > nanooctahedrons ≈ nanocubes > nanorods > nanooctahedrons. The BET (Brunauer, Emmett, and Teller) specific surface area and the particle size were the main factors affecting the Fenton catalytic activity. Moreover, the exposed {111} facets containing more Fe^{2+} species led to a stronger Fenton catalytic activity.

3.1.2. Peroxidase-mimic nanozymes based on Fenton-like reactions. The number of types of peroxidase-mimic nanozymes can be extended by applying Fenton-like reactions in addition to the Fenton reaction. By simply replacing iron atoms with other multivalent metal atoms such as Cu, Mn, Co, Ce, Ag, Cr, Ru, Mo, V, W, Ti, *etc.*, types of peroxidase-mimic nanozymes can be increased in vast numbers. Copper-based nanomaterials can be considered as the most common metal sources used in the Fenton-like reaction due to their low cost, high catalytic activity, and ease of modification in terms of shape, size, and terminal groups on the metal surface. The traditional copper-based peroxidase mimics simply use bulk copper ions in $CuSO_4$ or $CuCl_2$ solution as the catalyst for initiating Fenton-like reactions in the presence of H_2O_2. However, traditional copper-based reactions have some drawbacks such as low catalytic performance and instability in liquid form. The upgraded version of copper-based Fenton-like reactions focusses on achieving nano-size, at which quantum effects dominate, providing more accessible catalytic sites, leading to improved analytical performance. When the size of particles is around 1–100 nm, the materials' properties change significantly from those at larger sizes due to quantum effects. A powerful and fascinating result of quantum effects is the concept of tunable properties allowing scientists to literally fine-tune a property of a material *via* changing its size. In the Fenton/Fenton-like reaction, active sites on metals strongly affect their interaction with substrates. A higher number of active sites increases the availability of binding sites for H_2O_2, thereby increasing the rate of $^{\bullet}OH$ generation. Nanoscale metals contain more active sites and have higher specific areas as compared to bulk metals. Huang *et al.* synthesized a copper tannate (CuTA) nanolayer material, which was then used for colorimetric detection of H_2O_2.[55] The resultant CuTA contained a Cu–O–C structure, which was similar to the natural heme enzyme containing an Fe–N–C structure. CuTA exhibited a higher V_{max} (maximal reaction rate, 12×10^{-8} mM s^{-1}) and a lower K_m (Michaelis constant, 43.4 mM) than Fe_3O_4 ($V_{max} = 9.78 \times 10^{-8}$ mM s^{-1}; $K_m = 154$ mM), suggesting a higher catalytic efficiency compared to Fe_3O_4. The superior catalytic efficiency of CuTA originates from its nano-structure, which provides a higher number of accessible sites for H_2O_2 binding and enables efficient $^{\bullet}OH$ generation, leading to a faster and more pronounced chromogenic reaction. The LOD of this H_2O_2 colorimetric assay was as low as 6.15 μM.

In the conventional Fenton/Fenton-like reaction, metal ions and H_2O_2 need to be stored separately to prevent premature reactions because they react immediately upon contact with each other. This issue increases costs and complicates assay preparation. Recently, Lin *et al.* provided a feasible method to synthesize a copper peroxide (CP) nanodot through coordinating H_2O_2 to Cu_2O nanoparticles with the aid of polyvinylpyrrolidone (PVP) and NaOH.[56] NaOH plays a key role in deprotonating H_2O_2, facilitating the coordination of H_2O_2 with Cu^{2+}. The CP nanodot integrates both H_2O_2 and Cu^{2+} into a single nanostructure, thus addressing the issue of separate reagent storage. The CP nanodot can release H_2O_2 and Cu^{2+} to trigger Fenton-like reactions upon adding acid to neutralize NaOH. Although this technique has not been applied in colorimetric assays, the CP nanodot can become a great strategy for developing more feasible, more cost-effective, and simpler Fenton-like reaction-based colorimetric assays.

Colorimetric assays applying a Fenton-based peroxidase can be used to detect a wide range of targets including nucleic acids, proteins, biomarkers, insecticides, antibiotics, organic compounds, metal ions, *etc.* The large variants of Fenton-like reactions depending on changing their nanocomposite enable Fenton-based colorimetric detection with a large number of target types. Liang *et al.* used a MoO_3–Cu^{2+} system, in which MoO_3 acted as a co-catalyst for enhancing peroxidase activity in creatinine assay.[13] The MoO_3–Cu^{2+} complex facilitated the oxidation of TMB and had high selectivity for creatinine because its chemical and physical properties facilitated a specific binding effect toward creatinine. Each nanocomposite seems to have specific affinity for its respective substrate. Ray *et al.* demonstrated that gold nanoparticles confined in the wall of mesoporous silica (AuMS) had high affinity toward dopamine.[57] Among various biomolecules in the human body such as glucose, tryptophan, phenylalanine, tyrosine, ascorbic acid, and uric acid, only dopamine inhibits the Fenton-based oxidation of TMB, resulting in quenching of the blue color. To further increase the specificity of the Fenton/Fenton-like reaction, the surface of metal nanostructures can be conjugated with bio-recognition elements such as antibodies, aptamers, peptides, and molecular imprinted polymers (MIPs). This ensures that the Fenton/Fenton-like reaction occurs preferentially in the presence of specific target molecules, enhancing the specificity of the colorimetric biosensors. For example, Ali *et al.* conjugated an aptamer to Au@Fe_3O_4 nanoparticles.[58] The specific conformation of the aptamer endowed the Au@Fe_3O_4 nanoparticles with high affinity to *E. coli* O157:H7. Upon *E. coli* O157:H7 binding, Au@Fe_3O_4 nanoparticles cannot stimulate the Fenton/Fenton-like reaction, resulting in a significant decrease in absorbance. The specificity of aptamer-conjugated Au@Fe_3O_4 nanoparticles toward *E. coli* O157:H7 was demonstrated by evaluating their binding affinity against other pathogenic strains, including *S. aureus*, *K. pneumoniae*, *P. aeruginosa*, *L. monocytogenes*, *S. typhimurium*, *C. albicans*, and various *E. coli* serotypes (O78:H11, O1, O2, O6, O26, O33, O78, and O111). As a result, only *E. coli* O157:H7 inhibited the Fenton/Fenton-like reaction of Au@Fe_3O_4 nanoparticles.

In nanocomposites, the synergistic effect of multi-metal complexes is commonly used for enhancing the catalytic performance. Multimetallic nanozymes generally possessed greater catalytic activity than that obtained from monometallic or bimetallic nanozymes. For example, Au@PtRu nanorods exhibited much higher peroxidase-like activity than Au and Au@Pt nanorods.[60] PtPdCu trimetallic nanoalloys had enhanced peroxidase activity as compared to PtPd bimetallic nanoalloys and commercial Pt/C.[61] The insertion of Cu into the PtPd structure not only provides more active sites but also causes a change in the electronic structure, which is beneficial for improving the catalytic performance. $InCe_x$ nanoparticles possessed great peroxidase-like activity compared to pure In_2O_3

and CeO_2.[62] Su *et al.* demonstrated that $NiCo_2O_4$ mesoporous spheres enabled a lower limit of detection than the method using Co_3O_4 and NiO nanoparticles individually, highlighting the advantage of the bimetallic oxide over its single-metal counterparts.[63] Zhi *et al.* inserted Cu into three noble metals including Pt, Rh, and Ru to form a quaternary alloy nanozyme (PtRhRuCu), exhibiting peroxidase activity for a specific glucose assay (Fig. 2A).[59] The morphology of PtRhRuCu nanoparticles is shown in Fig. 2B. This nanocomposite possessed unique electronic structures and the modulation of the electronic states due to the multielement effect. The Cu ions were responsible for selective activation of Fenton-like reactions in the presence of H_2O_2 and regulation of the d-band center, which could obviously boost peroxidase activity. The PtRhRuCu nanoparticles show good selectivity for glucose detection, with minimal interference from other sugars (D-fructose, sucrose, D-galactose, and maltobiose), as shown in Fig. 2C. Moreover, the PtRhRuCu nanoparticles can detect glucose in the concentration range of 0 to 1 mM (Fig. 2D). The colorimetric assay applying the PtRhRuCu quaternary nanozyme can detect glucose as low as 0.98 μM, which is significantly lower than the limit of detection when using the PtRhRu ternary alloy nanozyme (29.59 μM).

One of the biggest disadvantages of Fenton and Fenton-like reactions is that metal ions are not stable in liquid solution and their catalytic activities are reduced over time, affecting the efficiency of colorimetric detection. For example, in a copper-based Fenton-like reaction, to initiate the generation of $^{\bullet}OH$, Cu^{2+} needs to be reduced to Cu^{+}; then, Cu^{+} mainly contributes to the catalytic reaction. However, Cu^{+} is unstable and easily oxidized to Cu^{2+} due to the low redox potential of Cu^{2+}/Cu^{+}. Moreover, the slow conversion of Cu^{2+} to Cu^{+} limits the reaction rate. To solve this problem, Hong *et al.* synthesized a catalyst that enables Cu to be in the reduced state (Cu^{+}), namely the 4-(dimethylamino) cinnamaldehyde oxalyl dihydrazone Cu(I) complex.[64] However, this complex only provides Cu^{+}, which does not assist the Cu^{2+}/Cu^{+} cycle. Later, Li *et al.* used fullerenes (C_{60})—a carbon-based nanomaterial—for dual purposes including stabilizing Cu^{+} and accelerating the Cu^{2+}/Cu^{+} cycle.[65] C_{60} can transfer electrons to Cu^{2+} and serve as a single electron acceptor of Cu^{0}, making C_{60} beneficial for stabilizing Cu^{+}.[66] The C_{60}-doped Cu^{+} exhibited impressive peroxidase activity resulting in excellent sensitivity with a detection limit of 115 nM bleomycin. The combination between metal ions and supports not only enhances the Fenton/Fenton-like reaction but also endows the catalysts with new features regarding the electrochemical signal output. For example, Song *et al.* used Cu^{2+}-doped polypyrrole nanotubes for dual-mode biosensors (colorimetric and electrochemical modes).[67] The polypyrrole

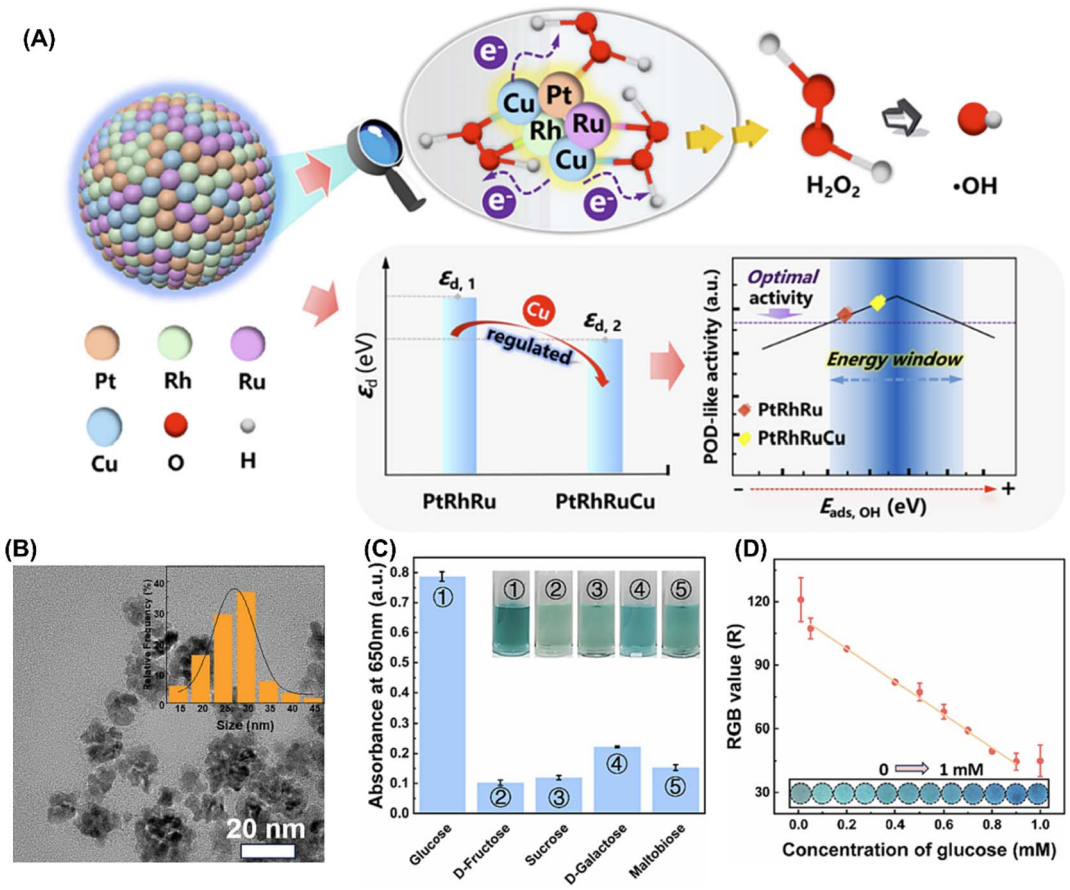

Fig. 2 (A) Mechanisms of enhanced peroxidase-like activity induced by the presence of Cu in a quaternary nanozyme. (B) TEM images of PtRhRuCu nanoparticles, containing size distribution. (C) Results showing the specificity test of glucose detection *via* PtRhRuCu-based colorimetric analysis. (D) Calibration curves of various glucose concentrations (0–1 mM; $y = -77.47557x + 113.18419$, $R^2 = 0.99893$).[59]

nanotubes with low dimensionality and a distinctive π-conjugated chain structure of the polymer provided high conductivity, while Cu^{2+} facilitated a Fenton-like reaction. As a result, this Cu^{2+}-doped polypyrrole nanotube biosensor had dual-signal outcomes including colorimetric and electrochemical signals.

3.2. MOF-assisted Fenton/Fenton-like reaction

Metal–organic frameworks (MOFs) are porous crystal coordination polymers with various pore sizes and functions. MOFs are self-assembled from metal ions and organic ligands *via* coordination action, endowing them with both inorganic and organic characteristics. MOF-based materials have been widely used in biosensors and catalysis due to their large specific surface area, abundant active exposure sites, favorable access of reactants to active sites, tailorable properties, *etc.* The ability for regular arrangement of metal nodes in MOFs endows MOF-based materials with peroxidase-like activity *via* catalyzing the Fenton/Fenton-like reaction.[68–71] Some MOF-based nanomaterials are constantly emerging in Fenton-based colorimetric biosensors, such as MILs,[72–74] PCNs,[75–77] ZIFs,[78–80] *etc.* Ren *et al.* used a MIL-53(Cu) support for immobilizing nFe_2O_3 nanoparticles (nFe_2O_3/MIL-53(Cu)).[81] nFe_2O_3/MIL-53(Cu) exhibited supreme catalytic activity due to better dispersion of nFe_2O_3, small size of particles, and the iron–copper synergistic effect. The nFe_2O_3/MIL-53(Cu)/H_2O_2 system reached a pseudo-first-order rate constant of 0.0123 min^{-1} for bisphenol A degradation, while MIL-53(Cu)/H_2O_2 and nFe_2O_3/H_2O_2 systems reached only 0.0026 and 0.0040 min^{-1}, respectively. This result revealed that MOFs could enhance the Fenton reaction.

One of the most useful strategies for enhancing the Fenton-based catalytic performance of MOFs is employing synergistic effects when multiple metals are used together. For example, Deng *et al.* employed synergistic effects by doping Mn and Fe ions along with Pd nanoparticles into Fe-MOF (Mn/Fe-MOF@$Pd_{1.0}$) for colorimetric detection of hydroquinone

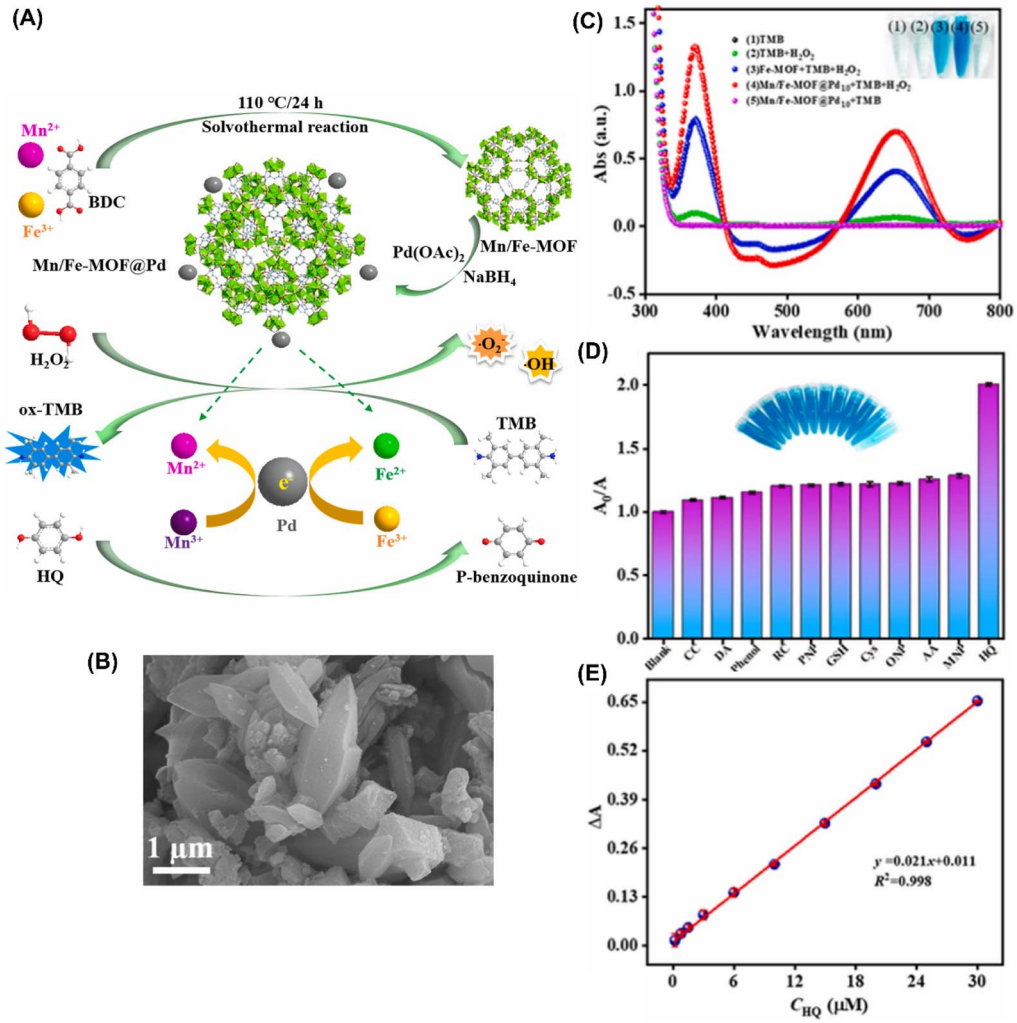

Fig. 3 (A) Solvothermal synthesis and synergistic Fenton/Fenton-like catalytic performance of the Mn/Fe-MOF@$Pd_{1.0}$ nanocomposite for the colorimetric detection of hydroquinone. (B) SEM image of Mn/Fe-MOF@$Pd_{1.0}$. (C) UV-vis absorption of different reaction systems demonstrating the enhanced catalytic activity of the Mn/Fe-MOF@Pd nanocomposite for the oxidation of TMB. (D) Selectivity of the Mn/Fe-MOF@$Pd_{1.0}$-based colorimetric biosensor for hydroquinone detection in the presence of various phenolic substances as interfering substances. (E) Linear relationship between absorption and hydroquinone concentrations.[82]

(Fig. 3A).[82] The morphology of Mn/Fe-MOF@$Pd_{1.0}$ is illustrated in Fig. 3B. In this system, Mn and Fe ions provide different redox potentials and work synergistically to activate H_2O_2 for producing active radicals, while Pd nanoparticles improve the structural stability and tolerance toward acidic conditions. Mn/Fe-MOF@$Pd_{1.0}$ oxidizes colorless TMB in the presence of H_2O_2 to form blue oxidized TMB (Ox-TMB). However, the presence of hydroquinone interferes with this chromogenic reaction, effectively maintaining TMB in its colorless form. Fig. 3C demonstrates that Mn/Fe-MOF@$Pd_{1.0}$ has significantly enhanced catalytic performance toward TMB oxidation compared to Fe-MOF alone. Moreover, the Mn/Fe-MOF@$Pd_{1.0}$ nanocomposite shows high selectivity for hydroquinone, with minimal interference from other structurally similar phenolic compounds (Fig. 3D). The Mn/Fe-MOF@$Pd_{1.0}$-based colorimetric biosensor showed a good linear relationship with hydroquinone concentrations ranging from 0.3 to 30 μM (R^2 = 0.998), with a detection limit of 0.09 μM (Fig. 3E). Similarly, bimetallic Fe/Co-MIL-88(NH_2) can convert colorless TMB to colored TMB at a higher reaction rate than the monometallic Fe-MIL-88(NH_2), resulting in the production of a 2.1 times higher signal.[83] In this system, Co(II) probably represents the reason for the enormous catalytic performance of Fe/Co-MIL-88(NH_2). Besides, the bimetallic MOF has higher affinities for both H_2O_2 and TMB as compared to the monometallic Fe-MIL-88(NH_2). The stronger affinity of the bimetallic MOF could be due to the highly porous nature of the MOF and the large number of active sites due to the presence of dual metals that strongly facilitate the binding and reaction with H_2O_2. For another example of multi-metallic MOFs, MoCu-2MI (2-methylimidazole) synthesized by Li *et al.* exhibited stronger peroxidase-like activity than pure Cu-2MI.[16] Mo served as a co-catalyst to accelerate the electron transfer and facilitated the Cu^{2+}/Cu^{+} cycle in the Fenton-like reaction. As a result, MoCu-2MI produced large levels of $^{\bullet}OH$ in the presence of H_2O_2 and finally improved the catalytic activity.

One of the most distinctive features of MOFs is their highly porous structure and the sizes of these pores can be easily controlled, which enables specific binding of targets. This feature not only enhances the specificity of colorimetric assays but also endows them with another function that is target separation and extraction. During the process of target separation, target molecules are drawn toward the MOF surface by diffusion from the bulk solution to the active pores of the MOF. This process occurs due to two types of intermolecular forces of attraction: (1) chemisorption (such as ionic interactions) and (2) physisorption (such as hydrogen bonding, van der Waals, and π–π interactions).[84,85] Some MOF-based materials that have been commonly used for target separation are MIL-101(Cr) for penicillin,[86] ZIF-8 for fluoroquinolones,[87] MOF-199 for benzene homologs,[88] MIL-53(Al) for PAHs,[89] $CoFe_2O_4$/MIL-101(Fe) for *N*-nitrosamines,[90] *etc.* Li *et al.* used Fe-NH_2-MIL-88B for both extraction and colorimetric detection of tetracycline.[15] The porous nature of Fe-NH_2-MIL-88B facilitated size-selective separation, while –NH_2 could react with –OH from tetracycline. More interestingly, the hydrogen-bonding interaction between –NH_2 and –OH caused electronic interactions that enhanced the Fenton reaction of Fe-NH_2-MIL-88B.

Some MOFs can contribute to the generation of fluorescence signals, making them valuable components in the design of dual-mode biosensors.[91,92] Combining fluorescence and colorimetric properties, MOFs serve as a promising approach for fabricating dual-mode biosensors. MIL-101(Fe)-NH_2 is a representative example, which can be synthesized by coordinating 2-aminoterephthalic acid (NH_2-BDC) as an organic ligand with $FeCl_3 \cdot 6H_2O$ as a metal node. NH_2-BDC incorporates a fluorescence emission peak at 455 nm when excited at 380 nm, while the mixed-valence metal node of Fe^{3+}/Fe^{2+} contributes to the Fenton reaction. This dual functionality enables MIL-101(Fe)-NH_2 to simultaneously generate both fluorescence and colorimetric signals. He *et al.* employed the bifunctionality of MIL-101(Fe)-NH_2@MIP for ratiometric fluorescent/colorimetric detection of chloramphenicol (CAP) (Fig. 4).[93] MIL-101(Fe)-NH_2@MIP catalyzed the oxidation of colorless *o*-phenylenediamine (OPD) to form a yellow solution of 2,3-diaminophenazine (DAP) in the presence of H_2O_2. In the meantime, the fluorescence intensity of MIL-101(Fe)-NH_2@MIP at 455 nm decreased, while the fluorescence of DAP at 560 nm increased under excitation at 380 nm. In the presence of CAP as a target molecule, the molecularly imprinted polymer (MIP) cavities on MIL-101(Fe)-NH_2@MIP capture CAP. This binding prevented H_2O_2 from entering the pores of MIL-101(Fe)-NH_2@MIP, thereby suppressing the Fenton reaction and reducing hydroxyl radical generation. As a result, catalyzed OPD chromogenic reactions are hindered, maintaining colorless OPD. Simultaneously, the fluorescence signal at 560 nm from DAP is suppressed, while the peak fluorescence signal of MIL-101(Fe)-NH_2@MIP at 455 nm is restored. Alternatively, Liu *et al.* reported a dual-mode biosensor for the early diagnosis of acute myocardial infarction (AMI) (Fig. 4B). Using cardiac troponin I (cTnI) as a diagnosis biomarker for AMI, they employed an ultrathin Fe-MOF-74 nanosheet, which exhibited both peroxidase-mimicking activity and fluorescence, to construct a biosensor capable of dual-mode detection of cTnI.[94] Upon cTnI binding, a cascade of reactions is triggered. First, glucose oxidase (GOx) is activated to generate hydrogen peroxide. Subsequently, ROS is produced through a Fenton-like reaction catalyzed by the generated hydrogen peroxide and Fe-MOF-74 nanosheet. ROS further changes colorless TMB into blue oxTMB. For the fluorescence signal, the Fe-MOF-74 nanosheet contains 2,5-dihydroxy-1,4-benzenedicarboxylic acid (DOBDC) ligands, which act as fluorophores with an excitation wavelength of 355 nm and an emission peak at 552 nm. The presence of cTnI increases the level of oxTMB, resulting in quenching fluorescence of the Fe-MOF-74 nanosheet. As a result, the fluorescence intensity decreases and is inversely proportional to the cTnI concentration. The biosensor showed good linearity with cTnI concentrations in the range of 10–2000 pg mL^{-1} in both fluorescence and colorimetric modes with the detection limits of 6.4 pg mL^{-1} and 8.4 pg mL^{-1}, respectively.

For target analysis, MOFs have become promising nanomaterials for assisting the Fenton/Fenton-like reaction to improve colorimetric biosensors due to the following advantages.

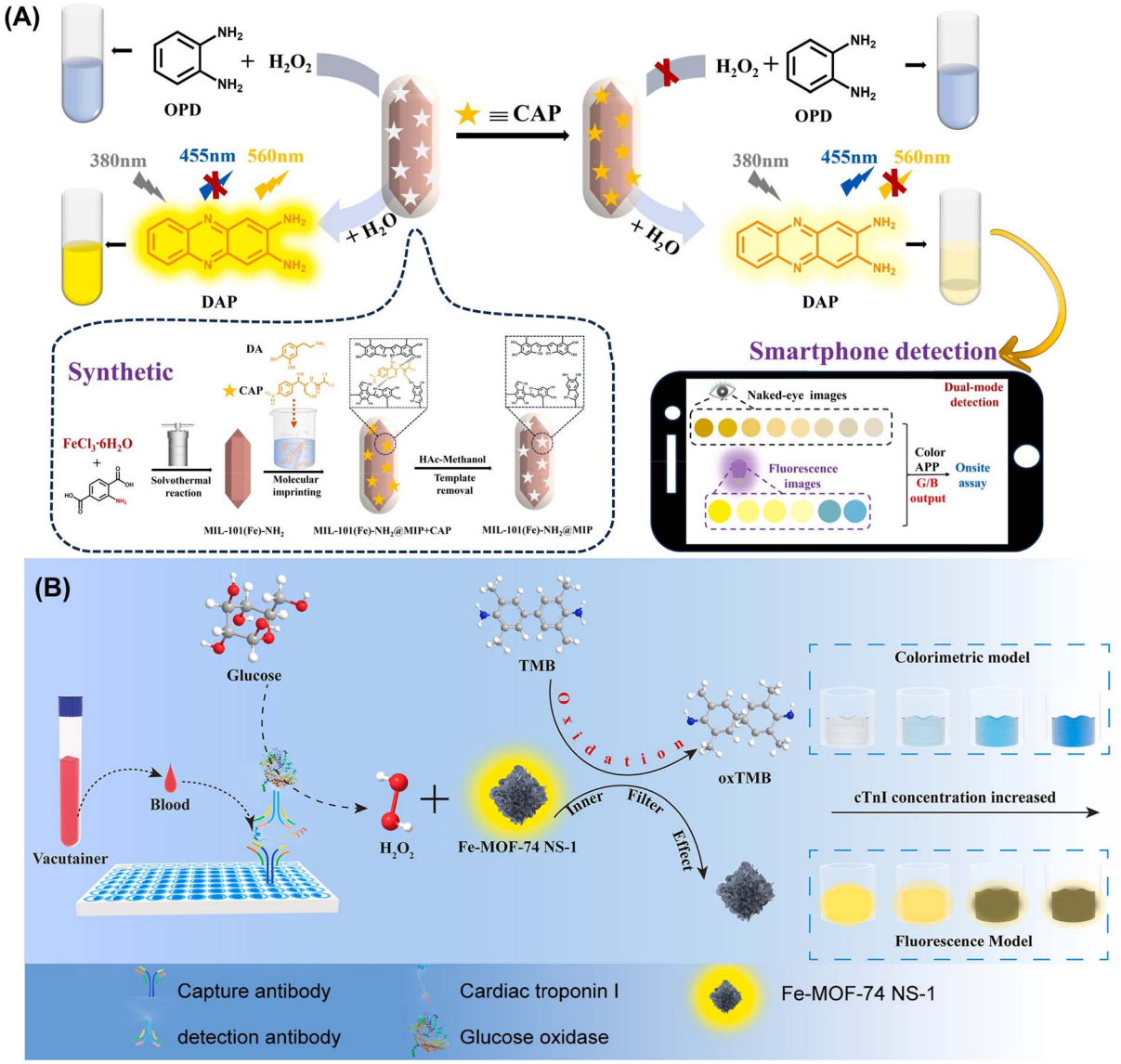

Fig. 4 (A) Schematic representation of colorimetric/ratiometric fluorescent dual-mode platform determination of chloramphenicol (CAP) *via* MIL-101 (Fe)-NH_2@MIP.[93] (B) Colorimetric/fluorescent detection of cardiac troponin I induced by Fe-MOF-74 NS-1.[94]

(1) *Tailorable porosity*: this feature offers the capability to control specific pore sizes and geometries for specific binding of target analytes. It results in enhanced selectivity and reduces interference from non-specific molecules. (2) *High specific surface area*: this feature provides a large interface for target binding, resulting in enhanced sensitivity of biosensors. (3) *Tunable surface functional groups*: various ligands, metal ions, aldehyde groups, carboxylic groups, and other functional groups can be selected to regulate appropriate interaction and affinity between MOFs and target analytes. (4) *Great biocompatibility and biodegradability*: the low toxicity of MOFs enables the development of biosensors for *in vivo* monitoring and target detection.

3.3. MXene-assisted Fenton/Fenton-like reaction

MXene is a new type of two-dimensional (2D) nanomaterial, which was first discovered when 2D titanium-carbide (Ti_3C_2) layers were exfoliated from bulk three-dimensional (3D) titanium aluminum carbide (Ti_3AlC_2) using hydrofluoric acid.[95] MXenes have the chemical formula $M_{n+1}X_nT_x$, where M implies transition metals (Cr, Mn, Ce, Ti, Mo, *etc.*); X implies either nitrogen or carbon; $n = 1$, 2, or 3; and T represents the functional groups (–O, –OH, and –F).[96] MXene has the suffix "ene" to indicate that it has graphene-like structures and shares the beneficial properties of graphene such as 2D architecture, great metallic conductivity, excellent adherence to substrates, large surface area, and fluorescence quenching ability. However, unlike graphene, MXenes show quick dispersion in aqueous media without the need for any additives. MXenes also contain more diverse functional groups resulting from the etching process. With these excellent properties, MXenes have become prospective materials for sensing applications. Unfortunately, MXenes alone cannot be used for colorimetric detection because pristine MXenes do not exhibit peroxidase-like activity

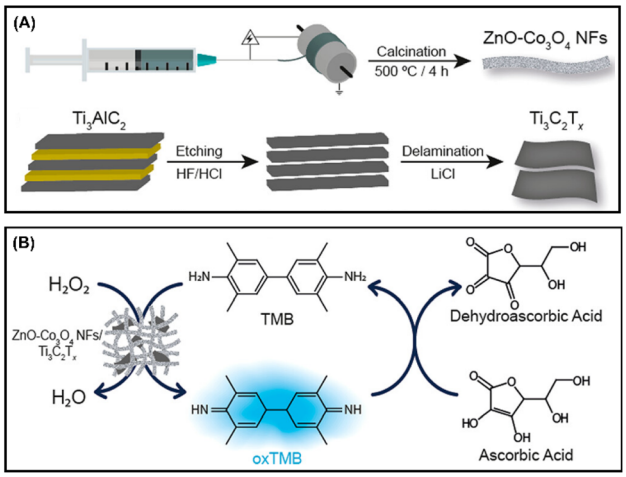

Fig. 5 (A) Synthesis and (B) application of a MXene-based nanocomposite for colorimetric detection.[18]

and cannot trigger the Fenton/Fenton-like reaction. Consequently, MXenes are not commonly able to change the color of chromogenic substrates. Therefore, MXenes are mostly used as supports for increasing the catalytic performance, stability, recyclability, pH, thermal resistance, *etc.* of the Fenton/Fenton-like reaction.

The ability of MXenes to improve the catalytic performance of the Fenton/Fenton-like reaction relies on the low valence transition metals surrounding the surface of MXenes. These low valence transition metals are considered as efficient reducing agents and can reduce Fe^{3+}, resulting in the facilitation of the Fe^{3+}/Fe^{2+} cycle. For example, the surface of Ti_3C_2 is filled with low valence titanium, which can trigger Fe^{3+}/Fe^{2+} redox cycling to activate H_2O_2 due to the ability to effectively reduce Fe^{3+} through Ti–C bond breakage.[96] Facure *et al.* demonstrated that the presence of Ti_3C_2 in ZnO–Co_3O_4 nanofibers led to a nanocomposite with superior catalytic activity.[18] The novel architecture formed when combining multiple types of nanomaterials probably promoted the synergistic effect. The van der Waals forces between Ti_3C_2 and ZnO–Co_3O_4 nanofibers can lead to more suitable conformations, which led to a nanocomposite with a higher specific surface area and a superior peroxidase-like activity. The Ti_3C_2 matrix has high electronic density and high electron mobility, which enhance rapid charge transfer

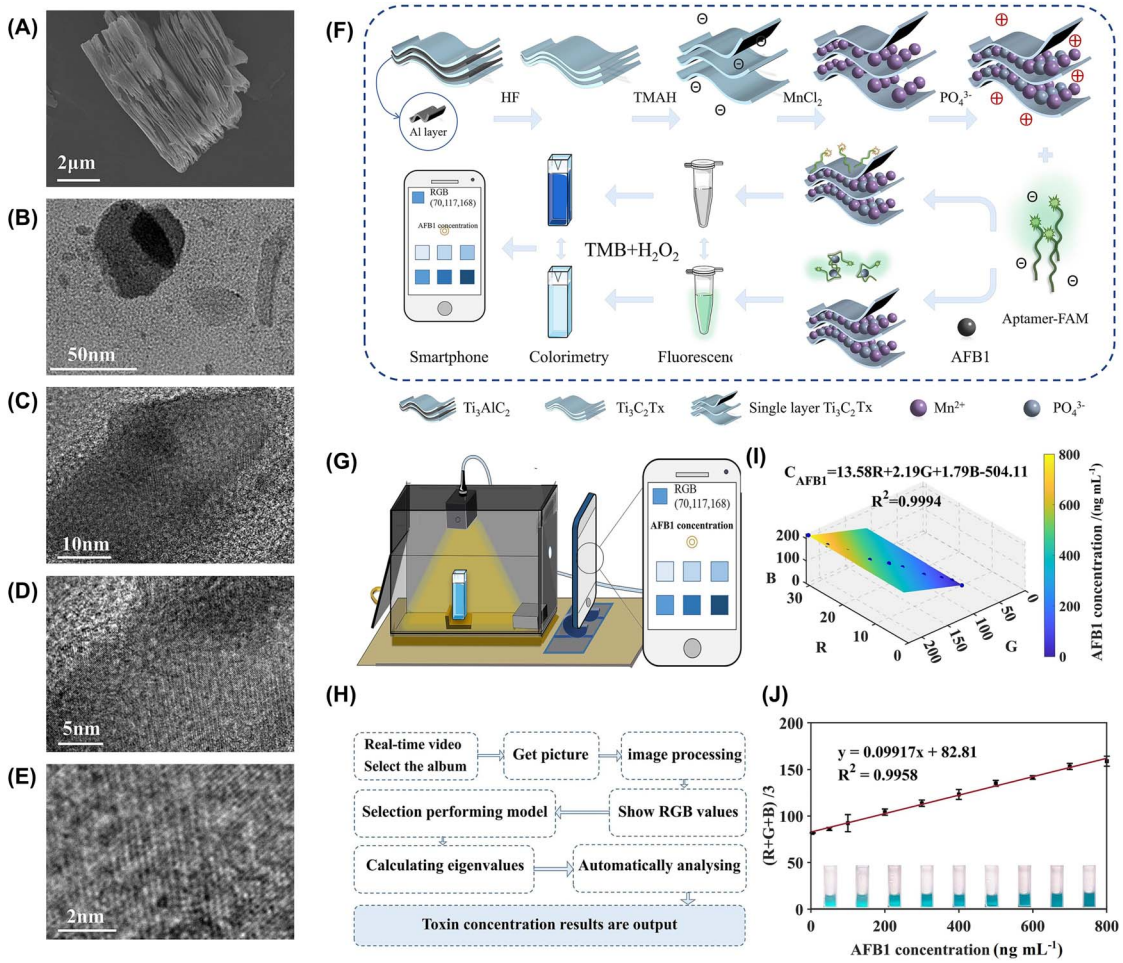

Fig. 6 (A) The SEM image of Ti_3C_2 MXene. (B–E) The TEM images of Ti_3C_2 MXene. (F) Preparation and application of Ti_3C_2@ssDNA for a multimode biosensor (colorimetric, fluorescence, and smartphone-based modes). (G and H) Design of a smartphone-based system for quantitative analysis. (I) Analysis of aflatoxin B1 concentration using the three channels of RGB. (J) Calibration curve showing the relationship between color intensity and aflatoxin B1 concentration in RGB mode.[106]

from TMB to H_2O_2. The 2D morphology of the Ti_3C_2 matrix provides a large surface area and great absorption ability, resulting in a boosted Fenton/Fenton-like reaction (Fig. 5A and B). Wang *et al.* used a Ti_3C_2@Fe_3O_4 nanocomposite to detect H_2O_2 with a detection limit of 0.4 μM.[97] The Ti_3C_2@Fe_3O_4 nanocomposite possessed a higher peroxidase-like activity than its individual components. The enhanced peroxidase-like activity of the Ti_3C_2@Fe_3O_4 nanocomposite was ascribed to the large ion-accessible interface, quick electron transfer channels in the MXene architecture, and the synergistic effect of Ti_3C_2 and Fe_3O_4.

Apart from Ti_3C_2, vanadium-based MXenes are other representative MXenes that can trigger the Fenton/Fenton-like reaction. V_2C MXene does not require the incorporation of other metals or metal oxides to promote the Fenton/Fenton-like reaction as Ti_3C_2. However, V_2C requires proper oxidation to be transformed into VO_xC before it can be used to trigger the Fenton/Fenton-like reaction.[98] In the chemistry of the VO_xC complex, vanadium has three adjacently mixed valence states: V^{3+}, V^{4+}, and V^{5+} in aqueous solution. Among these valence states, V^{4+} is dominant. This mixed valence state, dominated by V^{4+}, possesses abundant electron transport behaviors.[99]

Taking advantage of nanotechnology, transition metals have been controlled at the nanoscale level providing more active sites resulting in a more efficient Fenton/Fenton-like reaction. However, nano-sized metals are prone to aggregation due to the exponential increase of surface energy. The aggregation of nanoscale metals in aqueous solution significantly reduces the efficiency of the Fenton/Fenton-like reaction because it can block active sites resulting in instability and poor recyclability. In this regard, MXenes with layered structures serve as ideal substrates for anchoring catalytically active sites, thus increasing the stability of Fenton catalysts such as metals and metal oxides. The key that makes MXenes highly suitable for anchoring Fenton catalysts is the unique synthesis process of MXenes. Taking the most studied MXene as an example, Ti_3C_2 MXene is synthesized by selectively exfoliating the Al atom layers from the Ti_3AlC_2 precursor, followed by intercalation with dimethyl sulfoxide (DMSO). This process generates a unique accordion structure, which provides MXenes with more space for immobilization of Fenton/Fenton-like catalysts.[100] Some common metals and metal oxides coupled with MXene to form nanocomposites include Fe_3O_4/Ti_3C_2,[100] Cu_2O/Ti_3C_2,[101] Co_3O_4/Ti_3C_2,[102] $Cu_2O/TiO_2/Ti_3C_2$,[103] ZnO/Nb_2C, and ZnO/V_2C.[104] Fe_3O_4 anchored onto Ti_3C_2 MXene showed high recyclability over four cycles with high stability.[105] Meanwhile, $TiO_{1.47}$@C synthesized by direct oxidation of Ti_3C_2 MXene showed little change in the efficiency of Fenton-like reactions after five reactions, which demonstrates its high recyclability. The shelf life of $TiO_{1.47}$@C was highly desirable as it demonstrated good structural stability.[17] Another benefit of the etching process is that it could occasionally strip away transition metal atoms in MXenes leaving single vacancies or vacancy cluster defects that are highly oxophilic. These defect sites can easily form oxide clusters through abstraction of oxygen or hydrolysis. As a result, the compositing transition metals of MXenes such as V, Ti, and Nb can become source materials for the *in situ* formation of transition metal oxides. These multivalent metal oxides efficiently promote the Fenton/Fenton-like reaction in the presence of H_2O_2.

Moreover, MXenes not only enhance the efficiency of the Fenton/Fenton-like reaction for colorimetric detection, but also contribute to fluorescence-based detection due to their excellent fluorescence quenching properties. The dual properties

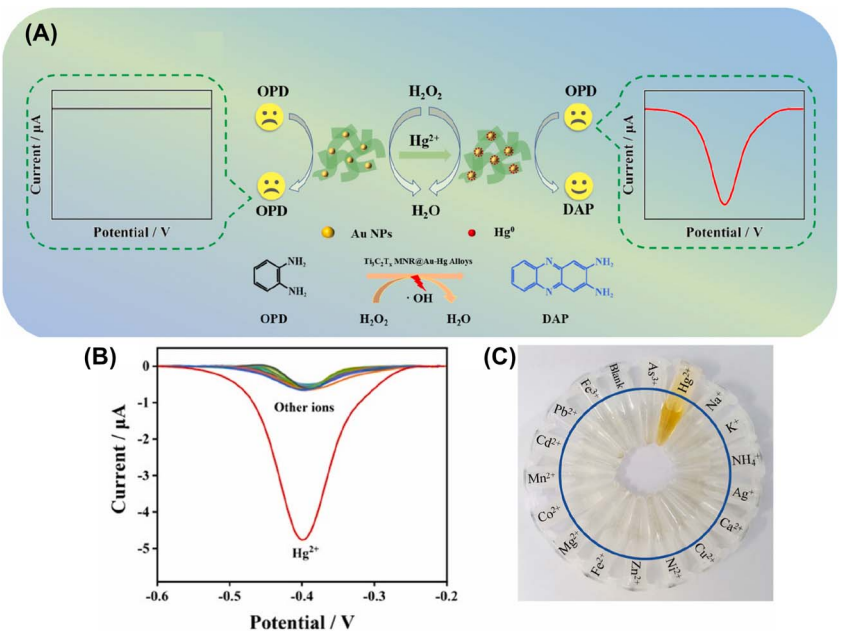

Fig. 7 (A) Mechanism underlying dual-mode (electrochemical/colorimetric mode) sensing of Hg^{2+} *via* the $Ti_3C_2T_x$ MNR@Au nanohybrid. (B) Differential pulse voltammetry (DVP) current response of different metal ions and Hg^{2+} added into the biosensor including Na^+, K^+, Ca^{2+}, NH_4^+, Cu^{2+}, Zn^{2+}, Ni^{2+}, Fe^{2+}, Co^{2+}, Mg^{2+}, Mn^{2+}, Pb^{2+}, Cd^{2+}, Fe^{3+}, and As^{3+}. (C) The corresponding image to the color change of different metal ions and Hg^{2+}.[108]

Table 1 Summary of the Fenton/Fenton-like reaction

Fenton reagent and dye	Type of nanomaterial	LOD	Target	Type of sample	Application
Fenton reagent: Fe_3O_4–Fe^0/Fe_3C, H_2O_2 dye: TMB[39]	Peroxidase nanozyme	67.1 pM	H_2O_2	Milk, live HepG2 cells	Food monitoring, cell monitoring
Fenton reagent: Fe_3O_4/nitrogen-doped porous carbon nanocomposite (Fe_3O_4/N-PCNC), H_2O_2 dye: TMB[41]	Peroxidase nanozyme	0.1 μM (H_2O_2) 2.6 μM (glucose)	H_2O_2, glucose	Various drinks	Food monitoring
Fenton reagent: Fe_3O_4@Pt nanoparticles, H_2O_2 dye: TMB[45]	Peroxidase nanozyme	0.36 μM (H_2O_2) 1.27 μM (glucose)	H_2O_2, glucose	Human serum samples, urine samples	Health monitoring
Fenton reagent: Ag–Fe_3O_4, H_2O_2 dye: TMB[46]	Peroxidase nanozyme	0.4 μM	Sulfur ions	Water	Environmental monitoring
Fenton reagent: PtRhRuCu quaternary alloy nanozymes, H_2O_2 dye: TMB[59]	Peroxidase nanozyme	0.021 mM	Glucose	Amino acid drink, probiotic drink, vitamin drink	Beverage monitoring
Fenton reagent: gold nanoparticles mesoporous silica (AuMS), H_2O_2 dye: TMB[57]	Peroxidase nanozyme	1.28 nM	Dopamine	Dopamine hydrochloride injection	Drug monitoring
Fenton reagent: Pt/Fe-MOF, H_2O_2 dye: TMB[109]	MOF	2.3 μM	Glucose	Human serum	Health monitoring
Fenton reagent: Fe/Co-MIL-88(NH_2) MOF, H_2O_2 dye: TMB[83]	MOF	7.8×10^4 particles per mL	Extracellular vesicles	Extracellular vesicles secreted by HeLa cells, sera samples	Health monitoring
Fenton reagent: Mn/Fe-MOF@$Pd_{1.0}$, H_2O_2 dye: TMB[82]	MOF	0.09 μM	Hydroquinone	Whitening cream and actual water samples	Environmental and cosmetic monitoring
Fenton reagent: MXene@Fe_3O_4, H_2O_2 dye: TMB[97]	MXene	0.4 μM (H_2O_2) 0.5 μM (glutathione)	H_2O_2, glutathione	Human blood samples	Health monitoring
Fenton reagent: VO_xC, H_2O_2 dye: TMB[99]	MXene	2.5 μM (dopamine) 0.36 μM (glutathione)	Dopamine, glutathione	Spiked solution	Health monitoring
Fenton reagent: Ti_3C_2, H_2O_2 dye: TMB[106]	MXene	0.09 ng mL^{-1} (fluorescent mode) 0.61 ng mL^{-1} (colorimetric mode) 0.96 ng mL^{-1} (smartphone mode)	Aflatoxin B1	Peanut sample	Food monitoring
Fenton reagent: ZnO–Co_3O_4 NFs/$Ti_3C_2T_x$, H_2O_2 dye: TMB[18]	MXene	0.58 μmol L^{-1}	Ascorbic acid	Orange juice	Beverage monitoring

regarding Fenton/Fenton-like catalysis and fluorescence quenching have made MXene nanocomposites become promising materials to fabricate dual-mode biosensors giving both colorimetric and fluorescent outputs. For example, Kong *et al.* used a Ti_3C_2 MXene nanozyme for the colorimetric and fluorescence dual-mode detection of aflatoxin B1 (Fig. 6). The morphology and nanostructure of the synthesized Ti_3C_2 MXene were characterized using SEM and TEM, as shown in Fig. 6A–E. Together, the SEM and TEM analyses confirm the typical layered morphology with an accordion-like structure of MXene. For fluorescence-based mode, the surface of Ti_3C_2 MXene was functionalized with a fluorescein (FAM) conjugated ssDNA aptamer (Fig. 6F). Ti_3C_2 MXene can absorb the emission energy of the FAM probe, resulting in the fluorescence quenching effect. However, the presence of the target aflatoxin B1 separates ssDNA aptamer-FAM due to the strong affinity between aflatoxin B1 and the ssDNA aptamer. Once the ssDNA aptamer-FAM structure left Ti_3C_2 MXene, its fluorescence emission was recovered. Meanwhile, colorimetric mode relied on the Ti vacancies, which were generated from the etching process in MXene synthesis. These Ti vacancies have high proton affinity and nucleophilicity, facilitating electron transfer from the surface of MXene to nearby H_2O_2 and further promoting the electron transfer from TMB to Ti_3C_2. When TMB loses electrons, the color of the solution changes from colorless to blue. The presence of the ssDNA aptamer effectively enhanced the activity of Ti_3C_2 MXene, while the dissociation of the aptamer due to the presence of aflatoxin B1 reduced the activity of Ti_3C_2 MXene. This dual-mode biosensor had detection limits of 0.09 ng mL^{-1} and 0.61 ng mL^{-1} for fluorescence and colorimetric modes, respectively. To further expand the application and increase the practicability of this biosensing strategy, a smartphone-based RGB analysis system was incorporated for quantitative analysis (Fig. 6G–I). After the colorimetric reaction catalyzed by Ti_3C_2 MXene through a Fenton-like mechanism, the results were captured using a smartphone under controlled lighting conditions for color intensity analysis. The Ti_3C_2 MXenes played a central role in this process, not only acting as peroxidase mimics but also facilitating the Fenton-like reaction. These MXene-driven Fenton-like reactions produced dual and reliable colorimetric outputs that varied with AFB1 concentrations. The MXene-based Fenton-like reaction combining a smartphone-based system showed a good linear relationship between RGB values and aflatoxin B1 concentrations in the range of 1–800 ng mL^{-1} (Fig. 6J).[106] Similarly, Nb_2C MXene coupled with aptamer-FAM was used to fabricate dual-mode (fluorescence and colorimetric) biosensors for the detection of aflatoxin B1.[107] This Nb_2C MXene-based dual-mode biosensor achieved a detection line as low as 0.0950 ng mL^{-1} under optimal conditions.

MXenes, with an accordion-like layered structure, provide a large surface specific area and abundant channels for electron transport. These unique properties make MXenes good candidates for fabricating dual-mode biosensors with both colorimetric and electrochemical outputs, especially when integrated with Fenton/Fenton-like reactions. This approach was effectively demonstrated in the work of Liu and co-worker (Fig. 7).[108] In their work, $Ti_3C_2T_x$ MXene nanoribbons were loaded with Au to form a $Ti_3C_2T_x$ MNR@Au nanohybrid *via* a simple self-reduction process and then used as a nanozyme to detect Hg^{2+}. The $Ti_3C_2T_x$ MNR@Au nanohybrid is extremely limited in triggering Fenton-like reactions. However, the presence of Hg^{2+} significantly enhances Fenton-like reactions of the $Ti_3C_2T_x$ MNR@Au nanohybrid, which can efficiently catalyze the oxidation of *o*-phenylenediamine (OPD) to form colored products (2,3-diaminophenazine, DAP) (Fig. 7A). Simultaneously, DAP produced a distinct reduction peak at −0.4 V, serving as an electrochemical signal. Based on this dual-mode approach, a highly sensitive biosensor was fabricated for the colorimetric and electrochemical detection of Hg^{2+}. The colorimetric mode enables convenient and naked-eye detection, while the electrochemical mode provides high sensitivity, with a detection limit as low as 17 pM and a wide linear range of 0.4 nM to 2 μM. The $Ti_3C_2T_x$ MNR@Au nanohybrid was demonstrated for high selectivity toward Hg^{2+} detection (Fig. 7B and C). This remarkable selectivity originates from the formation of an Au–Hg amalgam on the surface of the $Ti_3C_2T_x$ MNR@Au nanohybrid. The presence of Hg^{2+} significantly (Table 1) enhances the Fenton/Fenton-like reaction of the hybrid material, resulting in signal amplification that surpasses the response induced by other tested metal ions, including Na^+, K^+, Ca^{2+}, NH_4^+, Cu^{2+}, Zn^{2+}, Ni^{2+}, Fe^{2+}, Co^{2+}, Mg^{2+}, Mn^{2+}, Pb^{2+}, Cd^{2+}, Fe^{3+}, and As^{3+}.

4. Conclusion and future perspectives

This review summarized current reports discussing the mechanisms as well as current progress in the development and application of the Fenton/Fenton-like reaction for colorimetric biosensors. Along with significant advances in nanotechnology, the catalytic performance, stability, and recyclability of the Fenton/Fenton-like reaction have been significantly improved. First, from the perspective that the Fenton/Fenton-like reaction and peroxidase-mimic nanozymes are the two terminologies describing the same fundamental catalytic process, the advancements of nanozymes also increase the catalytic performance of the Fenton/Fenton-like reaction, especially for biosensor applications. For example, recent advances in nanozyme synthesis allow rational design of the active centers and the surface, which can control the catalytic performance of the Fenton/Fenton-like reaction. Second, MOFs assist the Fenton/Fenton-like reaction exhibiting supreme catalytic activity due to the ability to increase the dispersion of metals and metal oxides, resulting in smaller particles and more active sites. Besides, MOFs have a unique morphology with high porosity and the pore size can be easily adjusted. This feature enables MOFs to specifically capture analytes. Thus, by using a MOF-assisted Fenton/Fenton-like reaction, both sensitivity and selectivity of the colorimetric biosensors can be increased. Third, the MXene-assisted Fenton/Fenton-like reaction enables better stability and catalytic performance. MXenes with a layered structure serve as ideal substrates for anchoring catalytically active sites, thus increasing the stability of Fenton catalysts. The unique accordion structure of MXenes provides quick electron transfer channels and a large

ion-accessible interface in the MXene architecture, which eventually enhances the catalytic performance of the Fenton/Fenton-like reaction. Besides, MXenes have excellent fluorescence quenching properties, enabling the fabrication of dual-mode biosensors, which give both colorimetric and fluorescence outputs. However, some limitations remain to be overcome for further improvement.

First, although MOFs have been used for enhancing the selectivity of the Fenton/Fenton-like reaction through controlling pore sizes, the selectivity is still relatively low. Besides, optimization is required to find the pore size that offers the highest affinity toward the analytes which can cause extra cost and effort. Thus, future research needs to focus on improving selectivity as well as simplifying the optimization process. First, for enhancing selectivity, some current emerging technologies can be used such as molecular imprinting, aptamer conjugating, antibody/antigen coating, *etc.* Second, leveraging computer science can offer key benefits such as rational design for specific properties, a simple optimization process, discovery of Fenton/Fenton-like reaction pathways, *etc. via* simulation and computational modeling.

Second, the Fenton/Fenton-like reaction possesses multiple key features such as fast electron transfer cycles, strong catalytic performance, abundant sources of Fenton agents, *etc.* With these features, the Fenton/Fenton-like reaction can participate in several signal releasing pathways such as electrochemical, colorimetric, and fluorescent signals. Leveraging multiple signal releasing pathways, the Fenton/Fenton-like reaction possesses great potential for fabricating multiple-mode biosensors. There are several publications demonstrating the application of the Fenton/Fenton-like reaction for dual-mode biosensors. However, trio- and quad-mode biosensors have not been studied much yet. Future research should investigate more Fenton/Fenton-like nanocomposites that can release more types of signals for the fabrication of multiple-mode biosensors.

Third, the Fenton/Fenton-like reaction can produce hydroxyl radicals. These highly active species have strong antimicrobial activity, which can be employed for killing harmful microorganisms. The antimicrobial properties of the Fenton/Fenton-like reaction should be investigated and used together with biosensors to decrease the infectious risk from patients.

Data availability

No primary research results, software or code have been included, and no new data were generated or analysed as part of this review.

Conflicts of interest

There are no conflicts to declare.

Acknowledgements

This research was supported by the Vietnam National University, Ho Chi Minh City under grant number TX2025-50-01. The authors show their sincere gratitude to Tra Vinh University for generous support in this work. Also, the authors would like to gratefully acknowledge the Nguyen Tat Thanh University for support in this work.

References

1 L. Tessaro, A. Aquino, P. Panzenhagen, N. Joshi and C. A. Conte-Junior, *J. Pharm. Biomed. Anal.*, 2023, **222**, 115087.
2 A. Márquez, S. Santiago, M. V. Dos Santos, S. D. Aznar-Cervantes, C. Domínguez, F. G. Omenetto, G. Guirado and X. Muñoz-Berbel, *ACS Appl. Bio Mater.*, 2024, **7**, 853–862.
3 M. Adampourezare, B. Nikzad, S. Sajedi-Amin and E. Rahimpour, *BMC Chem.*, 2024, **18**, 80.
4 M. A. Redmile-Gordon, E. Armenise, R. P. White, P. R. Hirsch and K. W. T. Goulding, *Soil Biol. Biochem.*, 2013, **67**, 166–173.
5 S. Warakaulle, H. Mohamed, M. Ranasinghe, I. Shah, X. Yanyang, G. Chen, M. M. Ayyash, D. Vincent and A. Kamal-Eldin, *J. Food Compos. Anal.*, 2024, **126**, 105854.
6 G. M. Abu-Taweel, H. M. Al-Saidi, M. Alshareef, M. A. M. Alhamami, J. S. Algethami and S. S. Alharthi, *J. Fluoresc.*, 2025, **35**, 221–236.
7 Z.-P. Deng, B. Zhao, L.-L. Gao, B.-T. Ji, J.-G. Li, Y.-X. Sun, J. Li and Y. Sun, *J. Mol. Struct.*, 2024, **1299**, 137203.
8 C. Chen, Q. Fan, Z. Li, Z. Cai, Z. Ye and Y. Yin, *Nano Lett.*, 2024, **24**, 3737–3743.
9 C. Wenck, D. Leopoldt, M. Habib, J. Hegermann, M. Stiesch, K. Doll-Nikutta, A. Heisterkamp and M. L. Torres-Mapa, *Nanoscale Adv.*, 2024, **6**, 1447–1459.
10 J. Xiao, S. Guo, D. Wang and Q. An, *Chem.–Eur. J.*, 2024, **30**, e202304337.
11 A. A. Babu Christus, P. Panneerselvam and A. Ravikumar, *Anal. Methods*, 2018, **10**, 4378–4386.
12 H. A. Nguyen, H. Choi and N. Y. Lee, *Biosensors*, 2022, **12**, 488.
13 L. Liang, Y. Xiong, Y. Duan, W. Zuo, L. Liu, F. Ye and S. Zhao, *Biosens. Bioelectron.*, 2022, **206**, 114121.
14 X. Meng, Y. Xu, N. Zhang, B. Ma, Z. Ma and H. Han, *Sens. Actuators, B*, 2021, **338**, 129840.
15 Z. Li, F. Meng, R. Li, Y. Fang, Y. Cui, Y. Qin and M. Zhang, *Biosens. Bioelectron.*, 2023, **234**, 115294.
16 S. Li, L. Liang, L. Tian, J. Wu, Y. Zhu, Y. Qin, S. Zhao and F. Ye, *J. Mater. Chem. B*, 2023, **11**, 7913–7919.
17 Y. Jiang, D. Baimanov, S. Jin, J. Cheuk-Fung Law, P. Zhao, J. Tang, J. Peng, L. Wang, K. S.-Y. Leung, W. Sheng and S. Lin, *Proc. Natl. Acad. Sci. U. S. A.*, 2023, **120**, e2210211120.
18 M. H. M. Facure, L. A. Mercante, Y. Gogotsi and D. S. Correa, *ACS Appl. Nano Mater.*, 2025, **8**(9), 4291–4299.
19 R. E. Coleman, R. B. Boulton and A. A. Stuchebrukhov, *J. Phys. Chem. B*, 2023, **127**, 4300–4308.
20 R. Ovalle, in *Biochemistry*, ed, R. Ahmad, IntechOpen, 2022, vol. 28.
21 F. Haber and W. Joseph, *Proc. R. Soc. London, A*, 1934, **147**, 332–351.

22 S. Navalon, M. Alvaro and H. Garcia, *Appl. Catal., B*, 2010, **99**, 1–26.
23 B. Yuan, H.-L. Chou and Y.-K. Peng, *ACS Appl. Mater. Interfaces*, 2022, **14**, 22728–22736.
24 S. Guo and L. Guo, *J. Phys. Chem. C*, 2019, **123**(50), 30318–30334.
25 H. Dong, W. Du, J. Dong, R. Che, F. Kong, W. Cheng, M. Ma, N. Gu and Y. Zhang, *Nat. Commun.*, 2022, **13**, 5365.
26 Q. Ye, S. Ren, H. Huang, G. Duan, K. Liu and J.-B. Liu, *ACS Omega*, 2020, **5**, 20698–20706.
27 B. Bekdeşer and R. Apak, *ACS Omega*, 2024, **9**, 11738–11746.
28 R. Ai and Y. He, *Sens. Actuators, B*, 2020, **304**, 127372.
29 W. Cao, M. Jin, K. Yang, B. Chen, M. Xiong, X. Li and G. Cao, *J. Nanobiotechnol.*, 2021, **19**, 325.
30 Y. Liu and J. Wang, *Chem. Eng. J.*, 2023, **466**, 143147.
31 Y. Zhao, X. Deng, Y. Yang, Y. Zhang, H. Wang and B. Xin, *J. Environ. Chem. Eng.*, 2023, **11**, 110220.
32 S. Tang, H. Liu, E. Zhu, T. Zhao, Z. Wang, T. Jiao, Q. Zhang and D. Yuan, *Sep. Purif. Technol.*, 2022, **301**, 122056.
33 A. Ugartemendia, I. Casademont-Reig, L. Zhao, Z. Zhang, G. Frenking, J. M. Ugalde, A. Garcia-Lekue and E. Jimenez-Izal, *Chem. Sci.*, 2024, **15**, 6151–6159.
34 J. Guo, B. Gao, Q. Li, S. Wang, Y. Shang, X. Duan and X. Xu, *Adv. Mater.*, 2024, 2403965.
35 B. Das, J. L. Franco, N. Logan, P. Balasubramanian, M. I. Kim and C. Cao, *Nano-Micro Lett.*, 2021, **13**, 193.
36 C. Abe, T. Miyazawa and T. Miyazawa, *Molecules*, 2022, **27**, 5451.
37 L. Gao, J. Zhuang, L. Nie, J. Zhang, Y. Zhang, N. Gu, T. Wang, J. Feng, D. Yang, S. Perrett and X. Yan, *Nature Nanotech.*, 2007, **2**, 577–583.
38 N. N. Ulusu, *J. Mol. Evol.*, 2015, **80**, 251–257.
39 A. F. Baye, H. Thi Nguyen and H. Kim, *Sens. Actuators, B*, 2023, **377**, 133097.
40 A. Jonidi Jafari, B. Kakavandi, N. Jaafarzadeh, R. Rezaei Kalantary, M. Ahmadi and A. Akbar Babaei, *J. Ind. Eng. Chem.*, 2017, **45**, 323–333.
41 A. Nsabimana, S. A. Kitte, F. Wu, L. Qi, Z. Liu, M. N. Zafar, R. Luque and G. Xu, *Appl. Surf. Sci.*, 2019, **467–468**, 89–97.
42 V. Cao, P. A. Cao, D. L. Han, M. T. Ngo, T. X. Vuong and H. N. Manh, *Nat. Env. Poll. Tech*, 2024, **23**, 255–263.
43 Z. Duan, W. Zhang, M. Lu, Z. Shao, W. Huang, J. Li, Y. Li, J. Mo, Y. Li and C. Chen, *Carbon*, 2020, **167**, 351–363.
44 R. Zeng, Y. Li, X. Hu, W. Wang, Y. Li, H. Gong, J. Xu, L. Huang, L. Lu, Y. Zhang, D. Tang and J. Song, *Nano Lett.*, 2023, **23**, 6073–6080.
45 Y. He, P. Wang, X. Chen, Y. Li, J. Wei, G. Cai, K. Aoyagi and W. Wang, *R. Soc. Open Sci.*, 2022, **9**, 220484.
46 Y. Wang, Y. Ding, Y. Tan, X. Liu, L. Fu and W. Qing, *J. Environ. Chem. Eng.*, 2023, **11**, 109150.
47 B. Han, H. Guan, B. Peng, Y. Zhang and Y. Liu, *Anal. Methods*, 2022, **14**, 4832–4841.
48 J. Zhu and Z. Nan, *J. Phys. Chem. C*, 2017, **121**, 9612–9620.
49 X. Huang, C. Xu, J. Ma and F. Chen, *Adv. Powder Technol.*, 2018, **29**, 796–803.
50 J. Xiao, J. Lai, R. Li, X. Fang, D. Zhang, P. Tsiakaras and Y. Wang, *Ind. Eng. Chem. Res.*, 2020, **59**, 12431–12440.
51 T. T. N. Le, H. B. Truong, L. Thi Hoa, H. S. Le, T. T. T. Tran, T. D. Manh, V. T. Le, Q. K. Dinh and X. C. Nguyen, *Heliyon*, 2023, **9**, e20466.
52 Y. Wang, H. Li, L. Guo, Q. Jiang and F. Liu, *RSC Adv.*, 2019, **9**, 18815–18822.
53 Y. J. Jang, V. K. H. Bui, P. T. Nguyen, Y.-C. Lee and M. I. Kim, *Chemosensors*, 2021, **9**, 219.
54 Y. Zhong, L. Yu, Z.-F. Chen, H. He, F. Ye, G. Cheng and Q. Zhang, *ACS Appl. Mater. Interfaces*, 2017, **9**, 29203–29212.
55 Y. Huang, H. Zhong, C. Jiang, J. Yang, J. Zhang, F. Zhao and C. Liu, *Particuology*, 2024, **84**, 126–135.
56 L.-S. Lin, T. Huang, J. Song, X.-Y. Ou, Z. Wang, H. Deng, R. Tian, Y. Liu, J.-F. Wang, Y. Liu, G. Yu, Z. Zhou, S. Wang, G. Niu, H.-H. Yang and X. Chen, *J. Am. Chem. Soc.*, 2019, **141**, 9937–9945.
57 S. Ray, R. Biswas, R. Banerjee and P. Biswas, *Nanoscale Adv.*, 2020, **2**, 734–745.
58 R. Ali, A. Alattar, R. Alshaman, A. Ghabban, S. Alanazi, H. Al-Brahimi, M. Alatwi, A. Jlawi, A. Albalawi, A. Moutair Awad Alatawi, B. Al Balawi, A. Al-Marwani and M. M. El-Wekil, *Food Chem.*, 2024, **443**, 138564.
59 X. Zhi, Q. Yang, X. Zhang, H. Zhang, Y. Gao, L. Zhang, Y. Tong and W. He, *Food Chem.*, 2024, **445**, 138788.
60 F. Lv, Y. Gong, Y. Cao, Y. Deng, S. Liang, X. Tian, H. Gu and J.-J. Yin, *Nanoscale Adv.*, 2020, **2**, 1583–1589.
61 Y. Mao, F. Jia, T. Jing, T. Li, H. Jia and W. He, *ACS Sustainable Chem. Eng.*, 2021, **9**, 569–579.
62 B. Liu, H. Ruan, C. Li, J. Yao, B. Wei, L. Wang, S. Ban and J. Xie, *New J. Chem.*, 2023, **47**, 18476–18484.
63 L. Su, W. Dong, C. Wu, Y. Gong, Y. Zhang, L. Li, G. Mao and S. Feng, *Anal. Chim. Acta*, 2017, **951**, 124–132.
64 Z. Hong, J. Zhong, D. Ding, S. Gong, L. Zhang, S. Zhao, X.-C. Shen, H. Liang and F.-P. Huang, *Dalton Trans.*, 2023, **52**, 6187–6193.
65 S. Li, Y. Pan, M. Li, S.-H. Li, S. Zhao and F. Ye, *Anal. Bioanal. Chem.*, 2024, **416**, 6021–6031.
66 J. Zheng, L. Huang, C.-H. Cui, Z.-C. Chen, X.-F. Liu, X. Duan, X.-Y. Cao, T.-Z. Yang, H. Zhu, K. Shi, P. Du, S.-W. Ying, C.-F. Zhu, Y.-G. Yao, G.-C. Guo, Y. Yuan, S.-Y. Xie and L.-S. Zheng, *Science*, 2022, **376**, 288–292.
67 N. Song, S. Chen, D. Tian, Y. Li, C. Wang and X. Lu, *Mater. Today Chem.*, 2020, **18**, 100374.
68 P. Wu, F. Gong, X. Feng, Y. Xia, L. Xia, T. Kai and P. Ding, *J. Nanobiotechnol.*, 2023, **21**, 185.
69 C. Gao, S. Chen, X. Quan, H. Yu and Y. Zhang, *J. Catal.*, 2017, **356**, 125–132.
70 S. Lu, L. Liu, H. Demissie, G. An and D. Wang, *Environ. Int.*, 2021, **146**, 106273.
71 H. Sohrabi, S. Ghasemzadeh, S. Shakib, M. R. Majidi, A. Razmjou, Y. Yoon and A. Khataee, *Ind. Eng. Chem. Res.*, 2023, **62**, 4611–4627.
72 L. Liu, J. Wang, J. Wang, J. Wu, S. Wu and L. Xie, *ChemistrySelect*, 2021, **6**, 7143–7149.
73 P. Huang, Q. Chang, G. Jiang, X. Wang, H. Zhu and Q. Liu, *Spectrochim. Acta, Part A*, 2023, **285**, 121943.
74 Y. Lu, T. Wang, C. Tang, Q. Niu and T. You, *New J. Chem.*, 2023, **47**, 21505–21512.

75 M. Xia, T. Liu and Y. Zhang, *Anal. Sci.*, 2021, **37**, 1023–1027.
76 J. Li, X. Yang, Q. Li, D. Yang, Q. Hu, Z. Zhong and Y. Yang, *Food Biosci.*, 2024, **59**, 103910.
77 Y. Wu, C. Ke, Z. Song, H. Zhu, H. Guo, H. Sun and M. Liu, *Analyst*, 2024, **149**, 935–946.
78 Z. Zhao, T. Lin, W. Liu, L. Hou, F. Ye and S. Zhao, *Spectrochim. Acta, Part A*, 2019, **219**, 240–247.
79 K. Yang, G. Chen, L. Wang, M. Guo, J. Xu, Y. Ma, Z. Luo, A. Zeng and Q. Fu, *New J. Chem.*, 2023, **47**, 4103–4112.
80 S. Wang, D. Xu, L. Ma, J. Qiu, X. Wang, Q. Dong, Q. Zhang, J. Pan and Q. Liu, *Anal. Bioanal. Chem.*, 2018, **410**, 7145–7152.
81 Y. Ren, M. Shi, W. Zhang, D. D. Dionysiou, J. Lu, C. Shan, Y. Zhang, L. Lv and B. Pan, *Environ. Sci. Technol.*, 2020, **54**, 5258–5267.
82 D. Deng, Y. Wang, S. Wen, Y. Kang, X. Cui, R. Tang and X. Yang, *Anal. Chim. Acta*, 2023, **1279**, 341797.
83 Q. Jiang, Y. Xiao, A. N. Hong, Z. Gao, Y. Shen, Q. Fan, P. Feng and W. Zhong, *ACS Appl. Mater. Interfaces*, 2022, **14**, 41800–41808.
84 M. Safari, in *Recent Trends in the Application of Metal–Organic Frameworks*, IntechOpen, 2024.
85 Z. Hasan and S. H. Jhung, *J. Hazard. Mater.*, 2015, **283**, 329–339.
86 C. Lin, S. Lirio, Y. Chen, C. Lin and H. Huang, *Chem.–Eur. J.*, 2014, **20**, 3317–3321.
87 J. Pang, Y. Liao, X. Huang, Z. Ye and D. Yuan, *Talanta*, 2019, **199**, 499–506.
88 X.-Y. Cui, Z.-Y. Gu, D.-Q. Jiang, Y. Li, H.-F. Wang and X.-P. Yan, *Anal. Chem.*, 2009, **81**, 9771–9777.
89 X.-F. Chen, H. Zang, X. Wang, J.-G. Cheng, R.-S. Zhao, C.-G. Cheng and X.-Q. Lu, *Analyst*, 2012, **137**, 5411.
90 P. Miralles, I. Van Gemert, A. Chisvert and A. Salvador, *J. Chromatogr. A.*, 2019, **1604**, 460465.
91 C. Lou, F. Yang, L. Zhu, Q. Sun, Y. Yang and J. Guo, *Colloids Surf., A*, 2023, **677**, 132398.
92 S. Zhang, H. Li, D. Yang and Y. Yang, *Talanta*, 2024, **280**, 126785.
93 X.-Y. He, Y. Wang, Q. Xue, W.-F. Qian, G.-L. Li and Q. Li, *Food Chem.: X*, 2025, **26**, 102322.
94 J. Liu, Y. Wang, W. Peng, B. Qiu, K. Wong and S. Hu, *Anal. Chim. Acta*, 2025, **1350**, 343800.
95 M. Naguib, M. Kurtoglu, V. Presser, J. Lu, J. Niu, M. Heon, L. Hultman, Y. Gogotsi and M. W. Barsoum, *Adv. Mater.*, 2011, **23**, 4248–4253.
96 S. Xu, C. Liu, X. Jiang, X. Wang, S. Zhang, Y. Zhang, Q. Wang, W. Xiong and J. Zhang, *J. Hazard. Mater.*, 2023, **444**, 130450.
97 J. Wang, W. Xu, L. Zhou, T. Zhang, N. Yang, M. Wang, X. Luo, L. Jin, H. Zhu and W. Ge, *Microchim. Acta*, 2022, **189**, 452.
98 H. Geng, X. Li, X. J. Gao, Y. Cong, Q. Liu, J. Li, Y. Guan, L. Wang and W. He, *Nano Today*, 2023, **52**, 101989.
99 H. Jia, Q. Liu, J. Si, Y. Chen, G. Zhou, H. Lan and W. He, *Nanoscale Adv.*, 2023, **5**, 5799–5809.
100 Y. Cui, D. Zhang, K. Shen, S. Nie, M. Liu, H. Huang, F. Deng, N. Zhou, X. Zhang and Y. Wei, *J. Environ. Chem. Eng.*, 2020, **8**, 104369.
101 H. Xia, B. Li, Y. Ye, S. Wang, A. Chen and R. K. Kankala, *Adv. Healthcare Materials*, 2024, **13**, 2303582.
102 Y. Liu, R. Luo, Y. Li, J. Qi, C. Wang, J. Li, X. Sun and L. Wang, *Chem. Eng. J.*, 2018, **347**, 731–740.
103 J. Yin, B. Ge, T. Jiao, Z. Qin, M. Yu, L. Zhang, Q. Zhang and Q. Peng, *Langmuir*, 2021, **37**, 1267–1278.
104 W. Zhou, B. Yu, J. Zhu, K. Li and S. Tian, *Appl. Surf. Sci.*, 2022, **590**, 153095.
105 M. Rethinasabapathy, G. Bhaskaran, B. Park, J.-Y. Shin, W.-S. Kim, J. Ryu and Y. S. Huh, *Chemosphere*, 2022, **286**, 131679.
106 Y. Kong, Y. Zhu, J. Song, Q. Liu, L. Song, X. Fei and X. Li, *Food Chem.*, 2023, **426**, 136645.
107 Y. Kong, Z. Li, L. Zhang, J. Song, Q. Liu, Y. Zhu, N. Li, L. Song and X. Li, *Biosens. Bioelectron.*, 2023, **242**, 115725.
108 T. Liu, R. Zhou, K. Wu and G. Zhu, *Anal. Chim. Acta*, 2023, **1250**, 340975.
109 J. Li, J. Zhao, S. Li, Y. Chen, W. Lv, J. Zhang, L. Zhang, Z. Zhang and X. Lu, *Nano Res.*, 2021, **14**, 4689–4695.